MATHEMATICAL BIOSCIENCES
AND ENGINEERING
Volume **8**, Number **1**, January **2011**

doi:10.3934/mbe.2011.8.171

pp. **171–182**

A NOTE ON THE USE OF INFLUENZA VACCINATION STRATEGIES WHEN SUPPLY IS LIMITED

Sunmi Lee, Romarie Morales
and Carlos Castillo-Chavez

Mathematical, Computational and Modeling Sciences Center
School of Human Evolution and Social Change
Arizona State University
Tempe, AZ 85287, USA

Abstract. The 2009 A (H1N1) influenza pandemic was rather atypical. It began in North America at the start of the spring and in the following months, as it moved south, efforts to develop a vaccine that would mitigate the potential impact of a second wave were accelerated. The world's limited capacity to produce an adequate vaccine supply over just a few months resulted in the development of public health policies that "had" to optimize the utilization of limited vaccine supplies. Furthermore, even after the vaccine was in production, extensive delays in vaccine distribution were experienced for various reasons. In this note, we use optimal control theory to explore the impact of some of the constraints faced by most nations in implementing a public health policy that tried to meet the challenges that come from having access only to a limited vaccine supply that is never 100% effective.

1. **Introduction.** The World Health Organization (WHO) declared an influenza A(H1N1) pandemic on June 11, 2009 [17, 18], that is, just a few months after a novel strain had been identified from an infectious individual in Mexico [19]. The subsequent spread of this new strain of H1N1 in the southern hemisphere increased the fear that a more virulent strain would return to the northern hemisphere in the fall. Hence, efforts to develop a vaccine that could be distributed prior to the return of H1N1 to the northern hemisphere became a global priority. The uncertainties associated with the magnitude and nature of this health emergency dramatically increased the demand for a vaccine that was still in the design phase.

It soon became apparent that no more than 900 million vaccine dosages would be available in 2009-2010 [25]. Wealthy nations soon purchased most of the expected vaccine production leaving an inadequate supply available for the rest of the world. Canada for example ordered more than 50 million dosages while the USA secured 200 million dosages [20, 21]. On the other hand the WHO was able to secure only 37 millions dosages that had to be judiciously distributed to poor nations from December to February [26]. The first batches arrived in the USA on October 19 and in Canada on October 21, 2009 [22]. Limited supplies were used to vaccinate primarily pregnant woman, young children, and medical personnel [14, 23, 24]. In other words, nations that had managed to secure large supplies still had to

2000 *Mathematics Subject Classification.* Primary: 49J15, 49M05; Secondary: 92D25, 92D30.
Key words and phrases. Influenza pandemic, vaccine, optimal control, isoperimetric constraint.

wait several months for full delivery, with most dosages arriving well within the second wave. The challenge posed by vaccine production restrictions and logistic distribution limitations (experienced over the course of this pandemic) raised several questions: What is the impact of having access only to a limited number of dosages? What is the impact of delays in accessing the available vaccine supply? What is the role of a large percentage of H1N1 asymptomatic infectious individuals?

In this note, we only address the first question but its relationship to the others is addressed briefly in the conclusion. A single-outbreak epidemiological model is used to study the impact of a limited vaccine (not 100% effective) supply on the fall 2009-wave in the northern hemisphere. It is assumed (a highly conservative assumption) that the vaccine is available from the beginning of the outbreak. The role of this vaccine is first analyzed under the assumption that the population has access to an unlimited supply. Next, the case when the vaccine supply can only protect a small proportion of the total population at risk is studied numerically. In both cases, optimal control theory is used to find the optimal vaccine-strategy (unconstrained and constrained cases) in situations where the vaccine fails to protect a fraction of the vaccinated populations.

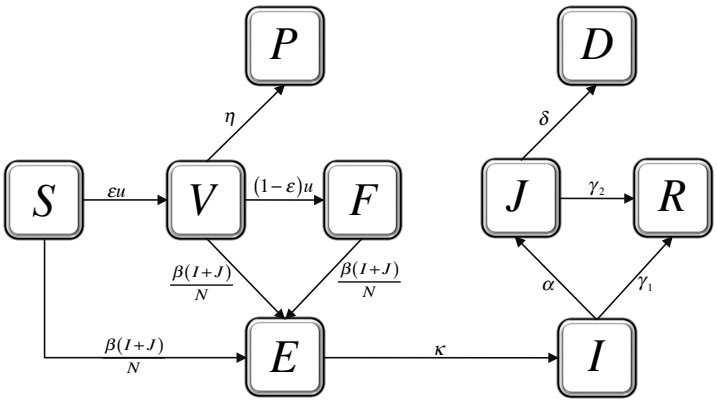

FIGURE 1. Flow chart of the single outbreak influenza transmission model with vaccination

2. **Pandemic influenza model with vaccination control.** In this section, we use an existing single outbreak model [2, 3] modified through the incorporation of a control function, the time-dependent vaccination rate. Two optimal control problems are formulated and their impact of (numerically derived) optimal vaccination strategies is evaluated under distinct vaccine coverage scenarios and various values of the basic reproduction number R_0. The model classifies individuals as susceptible (S), effectively vaccinated (V), ineffectively vaccinated (F), (perfectly) protected by vaccination (P), latent (E), infectious (I), hospitalized (J), recovered (R), and dead (D) (see Figure 1). Susceptible individuals are exposed to the influenza virus with a force of infection given by $\beta\frac{I(t)+J(t)}{N(t)}$ where β is the transmission rate and $N(t)$ denotes the total population size ($N(t) = S(t)+V(t)+F(t)+P(t)+E(t)+I(t)+J(t)+R(t)$). The control function (denoted by $u(t)$), the vaccination rate of susceptible individuals, is calculated under a particular set of assumptions. Susceptible individuals (S) go to the vaccination class

at the rate $\epsilon u(t)$, where ϵ in (0,1) is a measure of the vaccine efficacy. Therefore, $(1-\epsilon)$ denotes the fraction of ineffectively (failure) vaccinated individuals per unit of time. Vaccinated individuals go to the P (perfectly protected) class at the rate η while infected individuals enter either the Recovered class $R(t)$ at the rate γ_1 or the Hospitalized class $(J(t))$ at the rate α. Individuals in the Hospitalized class enter the Recovered class at the rate γ_2 or the Death $(D(t))$ class at the rate δ [3]. These definitions and assumptions lead to the following system of nonlinear differential equations that models the dynamics of a single epidemic outbreak.

$$\begin{aligned}
\dot{S}(t) &= -u(t)S(t) - \beta\frac{I(t)+J(t)}{N(t)}S(t) \qquad (1)\\
\dot{V}(t) &= \epsilon u(t)S(t) - \eta V(t) - \beta\frac{I(t)+J(t)}{N(t)}V(t)\\
\dot{F}(t) &= (1-\epsilon)u(t)S(t) - \beta\frac{I(t)+J(t)}{N(t)}F(t)\\
\dot{P}(t) &= \eta V(t)\\
\dot{E}(t) &= \beta\frac{I(t)+J(t)}{N(t)}(S(t)+V(t)+F(t)) - kE(t)\\
\dot{I}(t) &= kE(t) - (\alpha+\gamma_1)I(t)\\
\dot{J}(t) &= \alpha I(t) - (\gamma_2+\delta)J(t)\\
\dot{R}(t) &= \gamma_1 I(t) + \gamma_2 J(t)\\
\dot{D}(t) &= \delta J(t)\\
\dot{Y}(t) &= u(t)S(t)
\end{aligned}$$

The model's basic reproduction number R_0 (using the next generation operator approach [5, 16]) is given by

$$R_0 = \beta\left(\frac{1}{\alpha+\gamma_1} + \frac{\alpha}{(\alpha+\gamma_1)(\gamma_2+\delta)}\right). \qquad (2)$$

R_0 is a measure of the transmissibility of the infectious disease when the population is completely susceptible. Specifically, R_0 accounts for the average number of secondary cases generated by a primary case during his/her infectious period given that $S(0) \approx N(0)$. Typically, we have that when $R_0 > 1$ an outbreak takes place while $R_0 < 1$ indicates that an outbreak cannot be sustained. We take $S(0) = S_0$, $E(0) = E_0$, and $I(0) = I_0$ with $S_0 + E_0 + I_0 = N_0$ [$I_0 >$ and $E_0 > 0$ and $N_0 >> I_0 + E_0$]. Using the approach in [1], we derive the final size relationship

$$ln\frac{S_0}{S_\infty} < R_0[1 - \frac{S_\infty}{N_0}]$$

where the percentage of individuals recovered or dead from the infection is given by $[1 - \frac{S_\infty}{N_0}]$.

The aim of this work is to minimize the number of infected individuals over a finite time interval $[0, T]$ at a minimal cost. This outcome would be the result of implementing an optimal vaccine policy during the course of an influenza pandemic outbreak. These unconstrained (unlimited vaccines) and constrained (limited vaccines) optimal control problems are handled using the approach illustrated in

[8, 9, 10, 11]. The objective functional to be minimized is therefore

$$\mathcal{F}(u(t)) = \int_0^T [I(t) + \frac{W}{2}u^2(t)]dt \tag{3}$$

where the control effect is modeled by a quadratic term in $u(t)$. The weight constant W is a measure of the *relative* cost of vaccination over a finite time period. The constrained optimal problem with the isoperimetric-constraint (limited vaccine) consists of finding an optimal control function $u^*(t)$ such that

$$\mathcal{F}(u^*(t)) = min_{\Omega}\mathcal{F}(u(t)) \tag{4}$$

$$\int_0^T u(t)S(t)dt = B \tag{5}$$

where $\Omega = \{u(t) \in L^1(0,T) \| 0 \leq u(t) \leq b, t \in [0,T]\}$ and subject to System (1). The equality constraint (isoperimetric constraint) represents the total amount of vaccines available B over the time interval $[0,T]$. Constraint (5) can be reformulated in terms of the differential equation $\dot{Y}(t) = u(t)S(t)$ with the initial condition $Y(0) = 0$ and final condition $Y(T) = B$ (added to System (1)). This way of including the isoperimetric constraint lets us apply the standard Pontryagin's Maximal Principle in our search for an optimal solution of the constrained optimization problem (additional necessary conditions are derived in Appendix). The solution of the *unconstrained* optimal control problem excludes the $\dot{Y}(t)$ equation while the solution of the *constrained* problem requires the inclusion of the $\dot{Y}(t)$ equation which is equivalent to (5). The default values for initial conditions and model parameters are in Table 1. Units are per day for all rates. These baseline values are used throughout the manuscript unless otherwise indicated.

3. **Simulations and results.** We present numerical simulations under two scenarios: the unconstrained optimal vaccination and the constrained optimal one. The first case assumes that there exists a large vaccine supply to protect the (almost) full population while the later assumes that there is limited access to the vaccine. Our focus is on understanding the effects of optimal vaccination strategies on the dynamics of pandemic influenza. The impact of such controls is evaluated under different values of the basic reproductive number, R_0, and under pre-selected levels of vaccine coverage. A sensitivity analysis is carried out on the weight constants, on the upper bounds of the controls, and a mean vaccine efficacy in the unconstrained optimal vaccination strategy.

3.1. **Results in the unconstrained vaccine supply case.** First, the unconstrained optimal control problem is solved under two distinct transmissibility levels modeled by R_0. Figure 2 illustrates the optimal control functions computed (as a function of time) when $R_0 = 1.3$ and $R_0 = 2.0$ (top). The corresponding daily incidence of the infected class with/without vaccines is displayed in Figure 2 (bottom). The implementation of an optimal vaccine strategy reduces the number of infected cases significantly (almost no outbreak) when R_0 is low ($R_0 = 1.3$). We observe that maximum vaccination effort must be allocated at the beginning of the pandemic for both values of R_0. The optimal vaccination must be applied for a longer period of time when R_0 is high (R_0=2.0) since there are much more infected individuals (red solid curve in the top graph). In the absence of vaccines, a higher peak in the incidence of infected cases over a shorter time period is detected when $R_0 = 2.0$ (red dotted curve in the bottom graph). Even though a considerable increase in the

number of vaccines is put in place, there is still an outbreak (red solid curve in the bottom graph).

3.2. **Sensitivity analysis.** We explore the effect of changes in model parameters on the dynamics of influenza pandemics by carrying out a sensitivity analysis. Our sensitivity analysis focuses on studying the role of varying the control weight constants (W), the control upper bounds (the maximum vaccination rate), and the vaccine efficacy. The impact of these parameters on the fraction of cumulative infected cases is compared in the presence and the absence of vaccines.

Weight constant. We choose four values of the weight constants, $W = 1, 10^2, 10^4$, and 10^6 when $R_0 = 1.3$. A comparison of results implementing optimal vaccination policies is shown in Figure 3 under different weight constants on the control. Time series of optimal control functions are in the top of Figure 3 (left) while the corresponding incidence of infected individuals are in the bottom graph of Figure 3 (left). The general shapes of the control functions are similar (monotonic decreasing in time) with large changes in magnitude. As the weight constants are increased, the cost of vaccinations also increase. These changes result in increases in the height of the epidemic peak that are the result of reductions in the number of vaccines available to individuals. The impact of the weight constants on the fraction of cumulative infected cases and vaccinated cases is displayed as a function of R_0 in the right graph. Under higher vaccination coverage (almost 90% using the weight constants in the range of 10^2-10^6), the fraction of infected cases is reduced significantly (less than 10% of the total infected cases up to values of $R_0 <= 1.6$).

Upper bounds of the control. We carry out a sensitivity analysis on pre-selected control upper bounds starting from their impact on the fraction of cumulative infected cases. Four different upper bounds on controls (a priori maximum vaccination rates for susceptible individuals) are chosen in the range (0.05, 0.1, 0.2, 0.5). Figure 4 shows the results of implementing optimal vaccination controls constrained by these upper bounds when $R_0 = 1.3$. Optimal controls are graphed at the top while the corresponding incidence of infected individuals are plotted at the bottom (left). The cumulative fraction of infected and vaccinated cases are shown in the right graph of Figure 4 under different values of R_0. The larger upper bound, the better impact of vaccines in reducing the number of infected cases for all ranges of R_0 values. For example, the use of the largest upper bound ($b = 0.5$) generates dramatic reductions in the number of infected cases, regardless of the value of R_0.

Vaccine efficacy. We explore the impact of changes in vaccine efficacy on the control functions as well as on the fraction of cumulative infected cases. Figure 5 presents the results of implementing optimal vaccination strategies using different values for vaccine efficacy ($\epsilon = 0.4, 0.6, 0.8, 1$) when $R_0 = 1.3$. The optimal controls and the corresponding incidence of infected individuals are given in Figure 5 (left). It is observed that the vaccination strategy with larger vaccine efficacy uses less number of vaccines. For example, the amount of vaccines with an efficacy, $\epsilon <= 0.4$ is almost double of those required when $\epsilon >= 0.8$. The role of vaccine efficacy variation becomes clearer when one looks at the cumulative fraction of infected cases as R_0 is varied (Figure 5 right). The optimal vaccination strategy using a higher value of vaccine efficacy ($\epsilon = 0.8$) manages to keep the fraction of infected cases under 20% for most ranges of R_0 (< 2) even though it uses less vaccines.

3.3. **Results under Isoperimetric-constraint.** We solved a constrained (isoperimetric) optimal control problem under pre-specified isoperimetric constraints (amount

of vaccines). We consider three vaccine coverage levels (15%, 30%, and 50%). The numerical method used to solve this constrained optimal control problem turned out to be quite sensitive to the levels of vaccine available. As a result of the boundary conditions in the adjoint system (from the isoperimetric constraint), convergence issues had to be addressed.

Figure 6 plots time series of the optimal vaccinations under three different vaccine coverages (15%, 30%, and 50%). These results are contrasted with those obtained in the absence of vaccines. The left graph displays the control functions as well as the resulting incidence (infected cases) when a smaller value of the control upper bound (b=0.05) was in use. The right graph shows the results of using a larger value for the control upper bound (b=0.2). We see that maximum vaccination rates must always be implemented at the beginning until all the available vaccines are depleted in both cases. The effect of two upper control bounds on the incidence of infected cases does not seem to be significant provided that the maximum vaccination rates are put in place at the start of the pandemic and that R_0 lies in the low range (e.g $R_0 = 1.3$). The impact of vaccinations with 30% and 50% vaccine coverages on the fraction of cumulative infected cases is illustrated in Figure 7. When R_0 is low enough ($<= 1.4$), the optimal strategy with 30% still generates significant reductions ($<= 10\%$). However, the benefits of the application of controls under higher vaccine coverage ($>= 50\%$) increase as R_0 increases ($R_0 >= 1.5$).

4. **Conclusion.** An existing influenza transmission model is used to explore the impact of optimal vaccination policies under limited vaccine supplies (isoperimetric constrained model). Under a rather set of optimistic assumptions (vaccines available at the beginning of a pandemic), constrained and unconstrained optimal control problems are formulated. The constraint imposed (a limited vaccine supply) is incorporated in the isoperimetric optimal control problem through the addition of a differential equation with two "boundary" conditions.

Results suggest that both optimal vaccination policies (constrained or unconstrained) must be implemented at the maximum vaccination rate for all ranges of R_0 and at the beginning of the outbreak. There are no significant differences under the constrained or unconstrained strategies when R_0 is low ($<= 1.3$) and more in line with transmissibility estimates for seasonal influenza [4]. Hence, in some sense, this result indicates that there is no "need" for a nation to have more than 15 % of the vaccines needed to cover its total population. The pre-selected values of the upper bounds on controls and vaccine efficacy levels have a significant impact on the final size of infected cases. Increases on the upper bound of the optimal control and the efficacy level result in a decrease in the amount of vaccines that must be administered.

In this study, the focus has been exclusively in the study of constrained and unconstrained vaccine availability scenarios at the start of an epidemic outbreak. In other words, the study has been quite limited as noted in the introduction with important critical questions that should be simultaneously addressed being ignored. The time delays associated with the process of vaccine preparation, production and delivery of a new vaccine (around 6 months) just after a new strain was identified must be factored in. The role of age-specific risk, asymptomatic individuals (which can infect others) and the impact that these individuals have through their "accidental" use of vaccine supplies, must also be considered. These ignored factors make it difficult to mitigate the impact of super-fast spreading diseases like influenza. In

summary, for super-fast spreading diseases limitations in supply can make all the difference particularly when R_0 is large.

Appendix. The goal is to find an optimal vaccination strategy that minimizes the objective functional (3) subject to (1) and (4-5). The existence of optimal controls is guaranteed by standard results in control theory (the integrand of $\mathcal{F}$ is a convex function of u and the the state system satisfies the *Lipshitz* property with respect to the state variables) [6]. The necessary conditions that optimal solutions must satisfy are derived using Pontryagin's Maximum Principle [15]. This principle converts Systems (1) and (4) into minimizing the Hamiltonian H given by

$$\begin{aligned} H &= I(t) + \frac{W}{2}u^2(t) \\ &+ A_1(t)\{-u(t)S(t) - \frac{\beta}{N(t)}(I(t)+J(t))S(t)\} \\ &+ A_2(t)\{\epsilon u(t)S(t) - \eta V(t) - \frac{\beta}{N(t)}(I(t)+J(t))V(t)\} \\ &+ A_3(t)\{(1-\epsilon)u(t)S(t) - \frac{\beta}{N(t)}(I(t)+J(t))F(t)\} \\ &+ A_4(t)\{\frac{\beta}{N(t)}(I(t)+J(t))(S(t)+V(t)+F(t)) - kE(t)\} \\ &+ A_5(t)\{kE(t) - (\alpha+\gamma_1)I(t))\} \\ &+ A_6(t)\{\alpha I(t) - (\gamma_2+\delta)J(t)\} \\ &+ A_7(t)\{u(t)S(t)\} \end{aligned} \tag{6}$$

From this Hamiltonian and Pontryagins Maximum Principle, we obtain

Theorem 1. *There exist the optimal control $u^*(t)$ and corresponding state solutions, X^*= (S^*,V^*, F^*, P^*, E^*, I^*, J^*, R^*, D^*) that minimize $\mathcal{F}(u(t))$ over Ω. In order for the above statement to be true, it is necessary that there exist adjoint variables $A_i(t)$ such that*

$$\begin{aligned} \dot{A}_1 &= -[A_1(u(t) - A_1\frac{\beta}{N(t)}(I(t)+J(t)) + A_2(\epsilon u(t)) \\ &+ A_3((1-\epsilon)u(t) + A_4\frac{\beta}{N(t)}(I(t)+J(t)) + A_7u(t)] \\ \dot{A}_2 &= -[A_2 - \eta + A_2(-\frac{\beta}{N(t)}(I(t)+J(t))) + A_4\frac{\beta}{N(t)}(I(t)+J(t))] \\ \dot{A}_3 &= -[-A_3\frac{\beta}{N(t)}(I(t)+J(t)) + A_4\frac{\beta}{N(t)}(I(t)+J(t))] \\ \dot{A}_4 &= -[A_4(-k) + A_5k] \\ \dot{A}_5 &= -[1 - A_1\frac{\beta}{N(t)}S(t) - A_2\frac{\beta}{N}V(t) - A_3\frac{\beta}{N(t)}F(t) \\ &+ A_4\frac{\beta}{N(t)}(S(t)+V(t)+F(t)) - A_5(\alpha+\gamma_1) + A_6\alpha] \end{aligned} \tag{7}$$

$$\begin{aligned}\dot{A}_6 &= -[-A_1\frac{\beta}{N(t)}S(t) - A_2\frac{\beta}{N(t)}V(t) + A_3\frac{\beta}{N(t)}(F(t)) \\ &- A_4\frac{\beta}{N(t)}(S(t)+V(t)+F(t)) - A_6(\gamma_2+\delta)] \\ \dot{A}_7 &= 0\end{aligned}$$

satisfying the transversality conditions,

$$A_i(T) = 0,\ i = 1,\cdots,6 \tag{8}$$

$$A_7(T) = \theta. \tag{9}$$

The Hamiltonian H is minimized with respect to the control (at the optimal control). We differentiate H with respect to u on the set Ω and arrive at the following optimality condition:

$$\frac{\partial H}{\partial u} = Wu(t) - A_1(t)S(t) + \epsilon S(t)A_2(t) + (1-\epsilon)A_3(t)S(t) + A_7(t)S(t). \tag{10}$$

Solving for u^* (by evaluating $\frac{\partial H}{\partial u}$ at u^*), the optimality condition

$$u(t) = \frac{S(t)}{W}(A_1(t) - \epsilon A_2(t) - (1-\epsilon)A_3(t) + A_7(t)) \tag{11}$$

is obtained. Furthermore, using the standard argument for control bounds, we arrive at the following expression for the optimal control function

$$u^*(t) = min\big\{max\big\{0, \frac{S(t)}{W}(A_1(t) - \epsilon A_2(t) - (1-\epsilon)A_3(t) + A_7(t))\big\}, b\big\}. \tag{12}$$

The unconstrained solution can be computed by solving the optimality system which excludes the $\dot{Y}(t)$ equation in (1) and the $A_7(t)$ equation in (7). The standard two point boundary method is used to solve the unconstrained problem: first, the state system is solved using a forward method with given initial conditions; secondly, the corresponding adjoint system is solved using a backward scheme with the transversality conditions; thirdly, a convex combination of previously and currently computed controls are used to generate updated controls using the optimality equations; lastly, the process is repeated until a convergence criterion is satisfied.

For, the constrained optimization problem, a new state variable, $Y(t)$ is introduced in (1) from the isoperimetric constraint (5), which requires boundary conditions at $t = 0$ and $t = T$. From the requirements on $Y(t)$, the corresponding adjoint variable to $Y(t)$ must meet a non-zero transversality condition at the final time T, namely that $A_7(T) \equiv \theta$. Note that θ is unknown therefore, an iteration process is needed to find the right transversality condition required to satisfy the isoperimetric constraint ($Y(T) = B$). This additional iteration process uses Newton's method and the procedure used to implement it numerically identifies convergence issues that were never generated in the search of solutions for the unconstrained problem.

REFERENCES

[1] F. Brauer, Z. Feng and C. Castillo Chavez, *Discrete epidemic models*, Mathematical Biosciences and Engineering, **7** (2010), 1–15.

[2] G. Chowell, C. E. Ammon, N. W. Hengartner and J. M. Hyman, *Transmission dynamics of the great influenza pandemic of 1918 in Geneva, Switzerland: Assessing the effects of hypothetical interventions,* Journal of Theoretical Biology, **241** (2006), 193–204.

[3] G. Chowell, C. Viboud, X. Wang, S. Bertozzi and M. Miller, *Adaptive vaccination strategies to mitigate pandemic influenza: Mexico as a case study,* Public Library of Science, **4** (2009), e8164.
[4] G. Chowell, M. A. Miller and C. Viboud, *Seasonal influenza in the United States, France and Australia: Transmission and prospects for control,* Epidemiology and Infection, **136** (2007), 1–13.
[5] O. Diekmann and J. Heesterbeek, "Mathematical Epidemiology of Infectious Diseases: Model Building, Analysis and Interpretation," Wiley, 2000.
[6] W. H. Fleming and R. W. Rishel, "Deterministic and Stochastic Optimal Control," Applications of Mathematics, Springer Verlag, New york, 1975.
[7] R. Gani, H. Hughes, D. Fleming, T. Grifin, J. Medlock and S. Leach, *Potential impact of antiviral use during influenza pandemic,* Emerg. Infect. Dis., **11** (2005), 1355–362.
[8] E. Hansen and T. Day, *Optimal control of epidemics with limited resources,* Journal of Mathematical Biology, (2010), 1–29.
[9] E. Jung, S. Lenhart and Z. Feng, *Optimal control of treatments in a two-strain tuberculosis model,* Discrete and Continuous Dynamical Systems Series, **2** (2002), 473–482.
[10] S. Lee, G. Chowell and C. Castillo-Chavez, *Optimal control of influenza pandemics: The role of antiviral treatment and isolation,* Journal Theoretical Biology, **265** (2010), 136–150.
[11] S. Lenhart and J. T. Workman, "Optimal Control Applied to Biological Models," Chapman & Hall, CRC Mathematical and Computational Biology series, 2007.
[12] I. M. Longini Jr., M. E. Halloran, A. Nizam and Y. Yang, *Containing pandemic influenza with antiviral agents,* American Journal of Epidemiology, **159** (2004), 623–633.
[13] C. E. Mills, J. M. Robins and M. Lipsitch, *Transmissibility of 1918 pandemic influenza,* Nature, **432** (2004), 904–906.
[14] N. E. Basta, D. L. Chao, E. Halloran, L. Matrajt and I. M. Longini, Jr., *Strategies for Pandemic and Seasonal Influenza Vaccination of Schoolchildren in the United States,* American Journal of Epidemiolofy, **170** (2009), 679–686.
[15] L. S. Pontryagin, V. G. Boltyanskii, R. V. Gamkrelidze and E. F. Mishchenko, "The Mathematical Theory of Optimal Processes," Wiley, New Jersey, 1962.
[16] P. Van den Driessche and J. Watmough, *Reproduction numbers and sub-threshold endemic equilibria for compartmental models of disease transmission,* Mathematical Biosciences, **180** (2002), 29–48.
[17] World Health Organization (WHO), *Current WHO phase of pandemic alert for Pandemic (H1N1) 2009: Access 08/11/2009,* Available online: http://www.who.int/csr/disease/swineflu/phase/en/index.html.
[18] World Health Organization (WHO), *World now at the start of 2009 influenza pandemic: Update 06/11/2009,* Available online: http://www.who.int/mediacentre/news/statements/2009/h1n1_pandemic_phase6_20090611/en/index.html.
[19] Terra Mexico, *Mexico. Revelan que virus de influenza humana circulaba desde marzo: 05/05/2009 [In Spanish],* Available online: http://hygimia69.blogspot.com/2009/05/mexico-revelan-que-virus-de-influenza.html.
[20] Fox news, *40 Million Doses of H1N1 Vaccine Will Be Burned: Update 01/07/2010,* Available online: http://www.foxnews.com/story/0,2933,595724,00.html.
[21] CTV News, *Canada to lend Mexico 5M doses of H1N1 vaccine: Update 01/06/2010,* Available online: http://www.ctv.ca/servlet/ArticleNews/story/CTVNews/20100106/mexico_vaccine_100106/20100106.
[22] Health and Wellness, *H1N1 Vaccines available in Canada earlier than expected: 10/19/2009,* Available online: http://www.associatedcontent.com/article/2303283/h1n1_vaccines_available_in_canada_earlier.html.
[23] Health and Wellness, *H1N1 Vaccine approved in Canada: 10/21/2009,* Available online: http://www.associatedcontent.com/article/2311287/h1n1_vaccine_approved_in_canada.html?cat=5.
[24] The Wall Street Journal US, *Pregnant Women, Kids to Get Vaccine First: 07/30/2009,* Available online: http://online.wsj.com/article/SB124887563173290207.html.
[25] World Health Organization, *Update on A(H1N1) pandemic and seasonal vaccine availability: 07/07/2009,* Available online: http://www.who.int/immunization/sage/3.MPK-SAGE_7_July.pdf.

TABLE 1. Parameter definitions and baseline values (and their corresponding sources) used in numerical simulations.

Parameter	Description	Values	Reference
β	Transmission rate (days^{-1})	$0.75 - 1.68$	[2]
k	Rate of progression to infectious (days^{-1})	0.53	[13]
δ	Mortality rate (days^{-1})	0.01	[7]
γ_1	Recovery rate (days^{-1}) for infectious class (days^{-1})	0.34	[2]
γ_2	Recovery rate for hospitalized class (days^{-1})	1.10	[2]
α	Diagnostic rate (days^{-1})	0.51	[2]
ϵ	Efficacy of vaccination	0.5	[12]
$S(0)$	Initial number of susceptible individuals	174673	[2]
$E(0)$	Initial number of exposed individuals	207	[2]
$I(0)$	Initial number of infectious individuals	132	[2]
T	The simulated time (days)	200	-
b	The upper bound of control	$.05 - 0.2$	-
W	Weight constant on control	100	-

[26] Science Insider, *The Challenge of Getting Swine Flu Vaccine to Poor Nations: 11/03/2009,* Available online: http://news.sciencemag.org/scienceinsider/2009/11/the-challenge-o.html.

Received June 20, 2010; Accepted September 7, 2010.

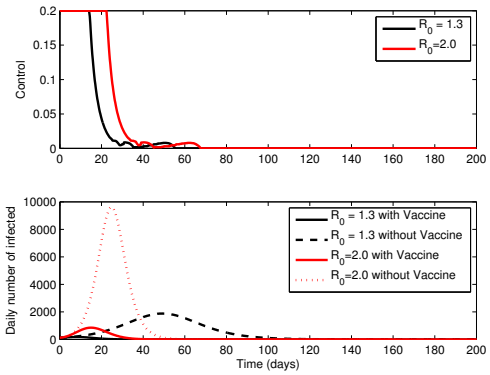

FIGURE 2. The optimal control functions over time are plotted when $R_0 = 1.3$ and $R_0 = 2.0$. The corresponding daily incidence rate in the infected class is compared to the situation in the absence of vaccines.

E-mail address: slee221@asu.edu
E-mail address: romarie.morales@asu.edu
E-mail address: ccchavez@asu.edu

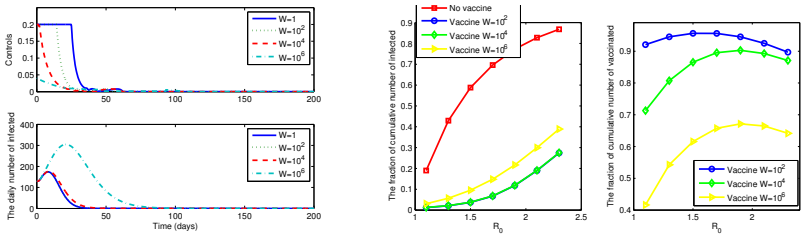

FIGURE 3. The comparison of results identifying optimal vaccination policies using different weight constants on the control ($W = 1, 10^2, 10^4, 10^6$) when $R_0 = 1.3$. The optimal controls and the corresponding incidence of infected individuals are illustrated (left). The fraction of the cumulative number of infected and vaccinated individuals are plotted under different weight constants as a function of R_0 (right).

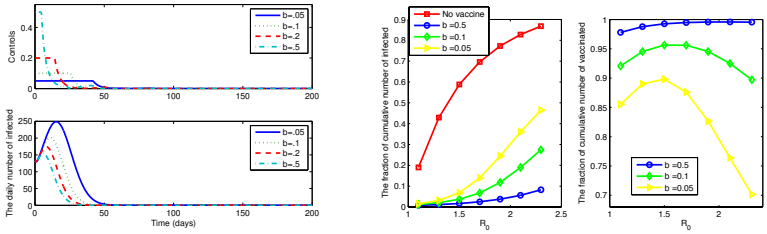

FIGURE 4. The results of implementing optimal vaccination strategies when different upper control bounds ($b = 0.05, 0.1, 0.2, 0.5$) are used with $R_0 = 1.3$. The optimal controls and the corresponding incidence of infected individuals are illustrated (left). The fraction of the cumulative number of infected and vaccinated individuals are plotted for distinct upper bounds as a function of R_0. (right).

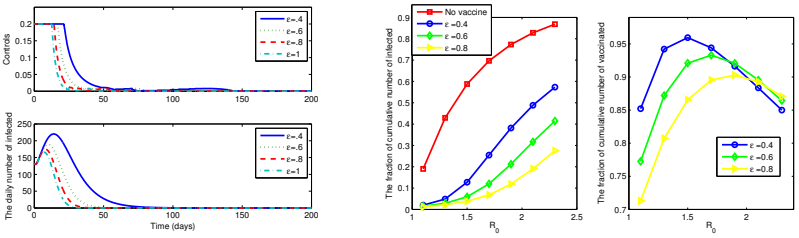

FIGURE 5. The results of implementing optimal vaccination policies under distinct vaccine efficacy constants on the control ($\epsilon = 0.4, 0.6, 0.8, 1$) when $R_0 = 1.3$. The optimal controls and the corresponding incidence of infected individuals are plotted (left). The fraction of the cumulative number of infected and vaccinated individuals are shown for different efficacy levels as a function of R_0 (right).

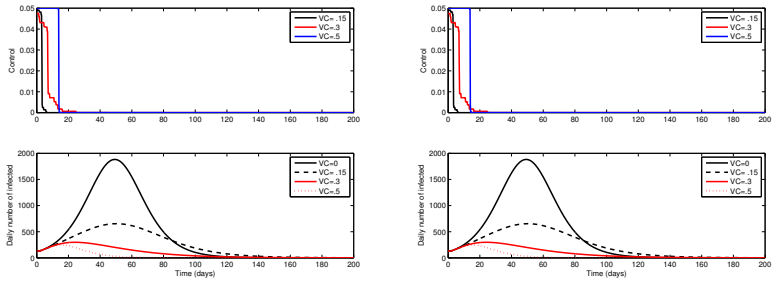

FIGURE 6. Optimal control functions are plotted when b=0.05 (left) and b=0.2 (right) under three different vaccination coverage (15%, 30%, and 50%). The corresponding daily incidence in the infected class is compared with the one in the absence of vaccines.

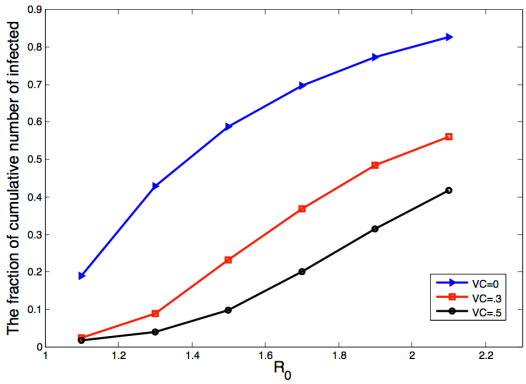

FIGURE 7. The fraction of the cumulative number of infected individuals as a function of R_0 is compared with the one under no vaccines using two different vaccination coverage levels (30% and 50%).